Topologically correct phase boundaries and transition temperatures for Ising Hamiltonians via self-consistent coarse-grained cluster-lattice models

Teck L. Tan[1,*] and D. D. Johnson[1,2,3,†]

[1]*Department of Materials Science and Engineering, University of Illinois at Urbana-Champaign, Urbana, Illinois 61801, USA*

[2]*Ames Laboratory, US Department of Energy, Iowa State University, Ames, Iowa 50011, USA*

[3]*Department of Materials Science and Engineering, Iowa State University, Ames, Iowa 50011, USA*

(Received 7 August 2010; revised manuscript received 22 December 2010; published 27 April 2011)

We derive a cluster mean-field theory for an Ising Hamiltonian using a cluster-lattice Fourier transform with a cluster of size N_c and a coarse-grained (CG) lattice into cells of size N_{cell}. We explore forms with $N_{cell} \geqslant N_c$, including a non-CG (NCG) version with $N_{cell} \to \infty$. For $N_c = N_{cell}$, the set of static, self-consistent equations relating cluster and CG lattice correlations is analogous to that in dynamical cluster approximation and cellular dynamical mean-field theory used in correlated electron physics. A variational N_c-site cluster grand potential based on $N_c = N_{cell}$ CG lattice maintains thermodynamic consistency and improves predictions, recovering Monte Carlo and series expansion results upon finite-size scaling; notably, the $N_c = 1$ CG results already predict well the first- and second-order phase boundary topology and transition temperatures for frustrated lattices. The NCG version is significantly faster computationally than the CG case and more accurate at fixed N_c for ferromagnetism, which is potentially useful for cluster expansion and quantum cluster applications.

DOI: 10.1103/PhysRevB.83.144427 PACS number(s): 64.60.De, 64.60.Cn, 64.75.Op, 75.10.Hk

I. INTRODUCTION

Cluster mean-field theories (CMFTs) are formulated and applied extensively in the study of material's phase transitions for classical Hamiltonians, i.e., the Ising model and cluster expansions.[1–5] Only for a few cases can the Ising model be solved exactly.[6] Generally, the partition function $Z[A]$ (with source fields A) and quantities such as site magnetization m_i and pair correlations G_{ij}, which dictate thermodynamic behavior, have to be approximated. CMFTs offer such an approximation but can differ greatly in their reliability, especially whether or not they maintain thermodynamic consistency. Notably, if the effects of the infinite lattice are not incorporated, CMFTs cannot properly predict phase transitions. A CMFT strategy is straightforward: A finite-size cluster containing N_c sites is treated (more) accurately, while the remaining sites in the infinite lattice outside the cluster interact via static mean fields, which consist of averaged quantities (e.g., m_i and G_{ij}) derived from the cluster partition function. Calculated correlations are local within the cluster and, for $N_c = 1$, the correlations are neglected, resulting in poor predictions of transition temperatures T_c, especially for frustrated systems.

For classical, static Hamiltonians, to improve on the prediction of cluster quantities, phase boundary topology, and T_c, we utilize the Dyson's equation that relates the pair correlations G of an N-site lattice with the self-energy Σ. We then enforce the consistency, which is neglected in most MFTs, between the coarse-grained (CG) lattice G (from Dyson's equation) and the cluster $\hat{G}$ evaluated from the cluster partition function (denoting cluster quantities with a hat). Although this consistency is easily enforced for $N_c = 1$, one has to consider the effect of boundary conditions on the consistency conditions for general sized clusters, which destroy the translational invariance of the lattice. For Ising models we adapt the CG and self-consistency concepts from quantum cluster methods, i.e., cellular dynamical mean-field theory (CDMFT)[7] and dynamical cluster approximation (DCA),[8] used in correlated-electron physics. Both methods use a cluster-lattice Fourier transform to invoke specific boundary conditions. The DCA enforces the same correlation length in real (**r**) space or Fourier (**k**) space by CG **k**-space integrals.[9] Notably, the DCA recovers the (static) coherent-potential approximation[10,11] for $N_c = 1$, and it is a proper generalization for $N_c > 1$, including for static, quenched disorder. So these same concepts can be applied to static classical thermodynamics. For correlated electrons, T_c are improved via scaling versus N_c,[12] which we also address.

From these concepts, the lattice can be CG into nonoverlapping cells of size N_{cell} sites and clusters of size N_c, where $N_{cell} \geqslant N_c$. We approximate the self-energy Σ with entries within (between) the cells being nonzero (zero). When $N_{cell} = N_c$ (which we call, for convenience, the DCA), the lattice G from Dyson's equation is coarse grained within a cell and is related self-consistently (one to one) to the cluster $\hat{G}$, permitting thermodynamic self-consistency to be obtained. We also explore a spectrum of $N_{cell} > N_c$ coarse-grained Ising MFTs.

The paper is organized as follows. Section II provides background on the Ising model and requirements for better MFT thermodynamics. With $N_c = 1$ DCA, the correct phase boundary topology and accurate T_c for a fcc antiferromagnet (AFM) is obtained already (see Fig. 1) because it satisfies thermodynamic self-consistency, manifested by the conservation of on-site correlations. In Sec. III, we generalize to multisite clusters, utilizing CG concepts and techniques to achieve self-consistency between lattice and cluster correlations, as well as thermodynamic consistency. Within the DCA we find a variational cluster grand potential, which we write in closed form. In Sec. IV, we apply DCA theory to determine T_c, phase boundary topologies, and scaling of T_c versus N_c via Betts' clusters,[13] comparing well with exact Monte Carlo (MC) results. We also investigate the computational efficiency and accuracy of other CG approaches where $N_{cell} > N_c$ at *small* N_c; a non-CG (NCG) version is obtained when $N_{cell} \to \infty$, which we show recovers a previous MFT.[14,15] For the ferromagnetic (FM) case, the NCG variant is computationally faster, more rapidly convergent versus cluster size, and accurate, which may be useful for quantum cluster and cluster expansion applications; however, in the AFM case, the NCG

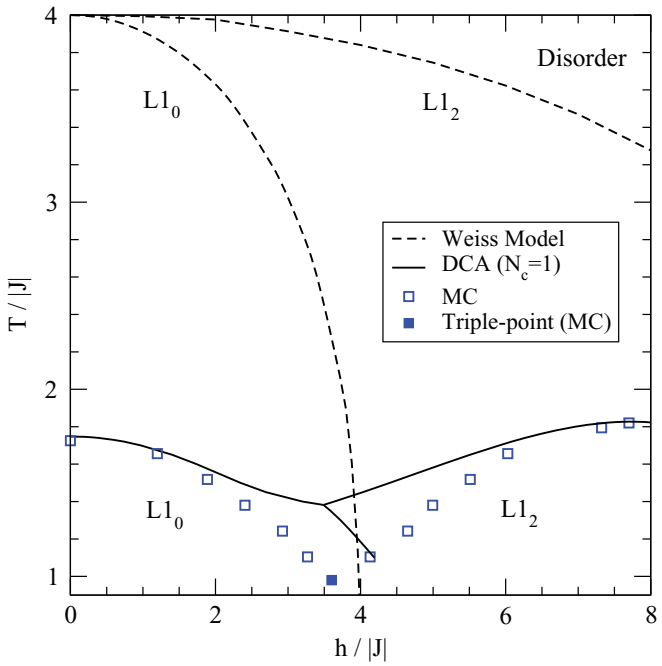

FIG. 1. (Color online) T-h boundaries for an fcc AFM. Diagram is symmetric about $h = 0$, so only $A1$, $L1_0$, and $L1_2$ are shown. Results are shown for MC (squares), Weiss[16,17] (dashed line), and the single-site MFT (solid line) that obeys (2b), also recovered via CG DCA at $N_c = 1$. Obeying (2b) improves T_c around stoichometry and gives the correct T-h topology.

method does not have a converged solution beyond $N_c = 1$ due to inconsistent boundary conditions.

II. BACKGROUND

To extend MFTs (e.g., Weiss,[16,17] Onsager,[18–20] and Brout[21,22]) to multisite clusters, we focus on the Ising Hamiltonian in a uniform field h, i.e.,

$$H = -\frac{1}{2}\sum_{i,j} J_{ij}\sigma_i\sigma_j - h\sum_i \sigma_i, \tag{1}$$

where $\sigma_i = \pm 1$ is the two-state spin variable on site i, with pairs of spins interacting via J_{ij}. We denote ensemble averages with $\langle\cdot\rangle$. Hence, the site magnetization is $m_i \equiv \langle\sigma_i\rangle$, and the pair (two-site) correlations are

$$G_{ij} = \beta^{-1}\chi_{ij} \equiv \langle\sigma_i\sigma_j\rangle - \langle\sigma_i\rangle\langle\sigma_j\rangle \tag{2a}$$

$$G_{ii} \equiv 1 - m_i^2 \tag{2b}$$

where $\beta^{-1} \equiv k_B T$ (k_B is Boltzmann's constant) and χ is the susceptibility. G_{ii} and m_i obey the sum rule in (2b), i.e., scattering intensity is conserved, because σ_i^2 and $\langle\sigma_i^2\rangle$ are 1. MFTs typically overly correlate, through self-interactions, the spins on two (or more) sites, such that (2b) is violated. Notably, G and H are always related, as shown by diagrammatic expansions;[23] that is, G satisfies a Dyson's equation relating the self-energy Σ, the irreducible part in the expansion, and J, i.e.,

$$\Sigma = G_0^{-1} - G^{-1}, \tag{3}$$

where $G_0^{-1} = -\beta J$, and all matrices are $N \times N$ for an N-site lattice (N is large). Given known J, the self-correlation G_{ii} from (3) satisfies (2b) only for the correct Σ.

The ensemble-averaged energy $E_{\text{avg}} = \langle H\rangle$ from (1) is expressed as single-site energy E_1 and *correlation energy* E_2, approximated (or ignored) in MFTs, i.e.,

$$E_{\text{avg}} = -\frac{1}{2}\sum_{i,j} J_{ij}m_i m_j - h\sum_i m_i - \frac{1}{2}\sum_{i,j} J_{ij}G_{ji}. \tag{4}$$

From (3), E_2, the last term in (4), can be written in terms of G and Σ as

$$E_2 = \frac{k_B T}{2}\text{Tr}(1 + G\Sigma). \tag{5}$$

In general, E_2 cannot be solved exactly, but it can be estimated within a finite cluster of size N_c while enforcing proper self-consistency of $\hat{G}$ and $\hat{\Sigma}$ in (3) via CG methods. The estimate approaches the exact result as $N_c \to \infty$.

A. Sum-rule requirement for CMFTs

For a single sublattice, the lattice G in (3) is diagonal in $\mathbf{k}$ space, giving $G(\mathbf{k}) = [-\Sigma(\mathbf{k}) - \beta J(\mathbf{k})]^{-1}$. Denoting translation between two lattice sites by $\mathbf{r}_{ij}$, we have

$$G_{ij} \equiv \frac{1}{V_{\text{BZ}}}\int d\mathbf{k} G(\mathbf{k})\exp(-i\mathbf{k}\cdot\mathbf{r}_{ij}), \tag{6}$$

where V_{BZ} is the volume of the first Brillouin zone (BZ). In cluster methods, the lattice Σ is divided into identical nonoverlapping cells with N_{cell} sites, with nonzero values for site indices belonging to the same cell and zero otherwise, while enforcing consistency between the *lattice* G and the *cluster* $\hat{G}$. In the limit of $N_c = 1$, Σ contains only diagonal entries; thus, G_{ii} in (6) must maintain particle number (2b) and concomitantly satisfy the Dyson's relation (3), which (for identical sites) becomes

$$G_{ii} = \frac{1}{\Omega_{\text{BZ}}}\int \frac{d\mathbf{k}}{-\Sigma_{ii} - \beta J(\mathbf{k})} = 1 - m_i^2. \tag{7}$$

Hence, there is a constraint on Σ_{ii}, as first discussed by Onsager[18] and later Brout,[21,22] which also provides the best initial (diagonal) guess of $\hat{\Sigma}$. More generally, for a multisite cluster, constraints are further required for off-diagonal elements within the cluster $\hat{\Sigma}_{ij}$, as initially approximated by Tokar.[15] In what follows we develop a CG CMFT that appropriately reflects the translational periodicity of the infinite lattice, and we invoke self-consistency conditions for the cluster, leading to dramatic improvement in quantitative prediction of transition temperatures and convergence with respect to N_c.

B. Cluster free energy

In phase-diagram calculations, free energies must be compared between possible states, and entropy S must be added to Eq. (4), giving $F = \bar{E} - TS$. With the usual definition of (grand) partition function, $Z[A] = \text{Tr}e^{-\beta H + A\sigma}$, where A is a source field vector (A_i applied to spin σ_i at site i). For all 2^N possible configurations on an N-site lattice, the grand potential is

$$\Omega[A] \equiv -k_B T \ln Z[A]. \tag{8}$$

Setting $A = 0$, the free energy is $F = \Omega[0]$. The one- and two-site state variables m_i and G_{ij} are

$$m_i = \frac{\partial \ln Z[A]}{\partial A_i}\bigg|_{A=0}, \quad G_{ij} = \frac{\partial^2 \ln Z[A]}{\partial A_i \partial A_j}\bigg|_{A=0}, \tag{9}$$

recovering both cases in (2). The second variation with respect to $\{m_i\}$ (Refs. 24 and 25) of the (Legendre transformed) grand potential $\Omega[A] + A \cdot m$ recovers (3), showing thermodynamic consistency; see also Sec. III B.

$Z[A]$ is exactly solvable for only a few cases. Direct evaluation of $Z[A]$ is often intractable for large N. Thus, in MFTs the partition function of a small N_c-site cluster embedded in the full lattice, $\hat{Z}[A]$, with 2^{N_c} configurations, is evaluated instead. Therefore, only state variables, such as m_i and G_{ij}, whose site indices are in the cluster, are configurationally averaged. When $\hat{Z}[A]$ further includes explicit dependence on self-energy (see the Appendix), any cluster evaluated $\hat{\Sigma}$ or $\hat{G}$ (from applying (9) to $\hat{Z}[A]$) has to be related consistently with the lattice Σ or G in (3), where Σ is divided into periodically repeating cells via CG. This thermodynamic consistency is key for lattice G to satisfy the sum rule in (2b) or the integral (or $\mathbf{k}$ space) version in (6) or (7), all of which can be generalized to multisublattice versions.

C. Sum-rule-conserving, single-site MFT

As a prelude to the self-consistency relations for general clusters, we summarize the simple improvement for $N_c = 1$, discussed in Sec. IV. First, we have the cluster $\hat{G}_{ii}$ and $\hat{\Sigma}_{ii}$, obtained from an appropriate cluster partition function,[15] $\hat{Z}[A]$ (see the Appendix), and the lattice G_{ii} and Σ_{ii}. When $\Sigma_{ii} = \hat{\Sigma}_{ii}$, $G(\hat{\Sigma}_{ii})$ from (3) is a functional of $\hat{\Sigma}_{ii}$ at fixed T and J. The value of $\hat{\Sigma}_{ii}$ is such that $G_{ii} = \hat{G}_{ii} = 1 - {m_i}^2$, satisfying (2b) and (7). The cluster $\hat{F}$ derived from $\hat{Z}[A]$ [see (28) and (33)] is used to determine the AFM phase boundary. We shall call this the sum-rule-conserving CMFT, which we show is recovered by CG lattice with $N_c = 1$. As shown in Fig. 1, the sum-rule-conserving CMFT gives the correct topology and good estimates of T_c at consulate points compared to "exact" lattice Monte Carlo simulations.

III. GENERALIZED CG CLUSTER MFT

For a multisite cluster approximation beyond single site ($N_c > 1$), the translational invariance of the original lattice is broken, and care is needed to relate lattice variables G and Σ from (3) to their counterparts $\hat{G}$ and $\hat{\Sigma}$ from the cluster $\hat{Z}[A]$. To the best of our knowledge, translational invariance and requirements between lattice and cluster variables have not been resolved completely, even though good estimates for the FM T_c had been demonstrated for the classical Ising model[15] for $2 \leqslant N_c \leqslant 4$. We use CG methods from DCA and CDMFT to account for cluster translational symmetry in the lattice and to obey (2) for $i, j \in$ cluster for G. We show that with a properly defined cluster $\hat{F}$ (see Sec. III E), reliable estimates for phase boundaries and T_c are obtained using finite clusters, yielding exact results via finite-size scaling as $N_c \to \infty$. Of course, the single-site case is recovered for $N_c = 1$ and provides rapid estimation of phase diagrams, as already suggested by Fig. 1. We emphasize that we utilize the coarse-graining from DCA and apply it to the Ising CMFT to ensure self-consistency between lattice and cluster quantities, which also results in thermodynamic consistency for the improved free energy.

A. CG methods from CDMFT and DCA

To distinguish between lattice and cluster variables, we refer to each partition of the lattice self-energy as "cell" (instead of cluster). To begin, the lattice self-energy is partitioned into nonoverlapping cells, $\tilde{\Sigma}$, containing $N_{\rm cell}$ lattice sites, where $N_{\rm cell} \geqslant N_c$, where, again, N_c is the number of cluster sites considered in $\hat{Z}[A]$. Hence,

$$\Sigma_{(i,I)(j,J)} = \tilde{\Sigma}_{IJ}\delta_{ij}, \tag{10}$$

where the double index denotes a site (out of a total of N sites) in the lattice, with capital $I(J)$ denoting sites within each cell $i(j)$.

Assuming identical cells, one can carry out an intercell Fourier transform on the lattice variables (see Fig. 2) using vectors $[\mathbf{a}_1, \mathbf{a}_2, \mathbf{a}_3]$, as opposed to translation vectors of the lattice $[\mathbf{A}_1, \mathbf{A}_2, \mathbf{A}_3]$. For a lattice variable X,

$$X_{IJ}(\mathbf{k}) = \frac{N_{\rm cell}}{N} \sum_{i,j} X_{(i,I)(j,J)} e^{i\mathbf{k}\cdot\mathbf{r}_{ij}}, \tag{11}$$

where $N/N_{\rm cell}$ is the total number of cells and the displacement between cells i and j is given by $\mathbf{r}_{ij}$, where $\mathbf{r}_{ij} = n_1\mathbf{a}_1 + n_2\mathbf{a}_2 + n_3\mathbf{a}_3$, with n_i being integers. Applying the intercell Fourier transform to (3),

$$G^{-1}_{IJ}(\mathbf{k}) = -\tilde{\Sigma}_{IJ} - \beta J_{IJ}(\mathbf{k}), \tag{12}$$

where the terms are entries to $N_{\rm cell} \times N_{\rm cell}$ symmetric matrices and $\tilde{\Sigma}_{IJ}$ is independent of $\mathbf{k}$. With no further assumptions (other than matrices are symmetric), $\tilde{\Sigma}$ will have

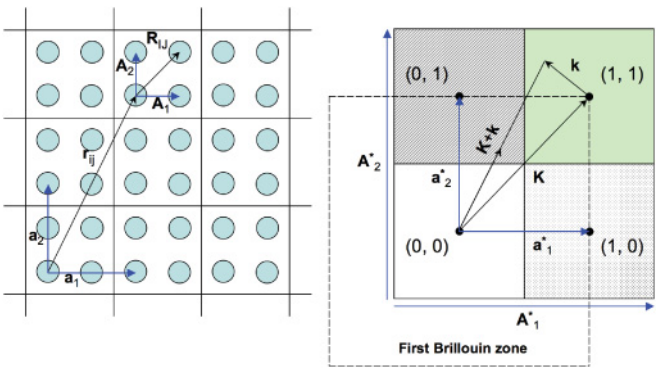

FIG. 2. (Color online) Coordinates describing the partition of the lattice into nonoverlapping cells, illustrated for $N_{\rm cell} = 4$ on a 2D square lattice. (left) Real-space translation vectors of the lattice sites and cells are $[\mathbf{A}_1, \mathbf{A}_2]$ and $[\mathbf{a}_1, \mathbf{a}_2]$, respectively, with R_{IJ} ($\mathbf{r}_{ij}$) being the vector between two intracluster (intercell) sites. (right) Corresponding reciprocal-space translation vectors of the lattice (cells) are $[\mathbf{A}^*_1, \mathbf{A}^*_2]$ ($[\mathbf{a}^*_1, \mathbf{a}^*_2]$). With $N_{\rm cell} = 4$ and when the cluster transform is done in a cell, there are four cluster momenta $\mathbf{K}_n$ in the first BZ volume $V_{\rm BZ}$, and their positions are generated by $[\mathbf{a}^*_1, \mathbf{a}^*_2]$. The vector $\mathbf{k}$, from the Fourier transform of intercell coordinates, is quasicontinuous at large N and is assigned to CG (shaded) regions with volume $V_{\tilde{\Delta}} = V_{\rm BZ}/N_{\rm cell}$.

$N_{\rm cell}(N_{\rm cell}-1)/2$ independent entries, and a violation of translational invariance within the cell is possible.

Translational invariance. If a given lattice variable is further required to be translational invariant within the cell, as in the DCA,[8] X_{IJ} is diagonal in the $\mathbf{k}$ space of the cell. Via the cluster transform,

$$X(\mathbf{K}_n) = \frac{1}{N_{\rm cell}} \sum_{IJ}^{N_{\rm cell}} X_{IJ} e^{i\mathbf{K}_n\cdot\mathbf{R}_{IJ}}, \tag{13}$$

where $\mathbf{K}_n$ are the $N_{\rm cell}$ cluster momenta in the BZ (illustrated in Fig. 2) and $\mathbf{R}_{IJ}$ is the displacement between sites I and J within the cell. The summation in (13) is restricted to sites within the cell. The $\mathbf{K}_n$ are points in $\mathbf{k}$ space produced by the reciprocal vectors of the cell $[\mathbf{a}_1^*,\mathbf{a}_2^*,\mathbf{a}_3^*]$, where $\mathbf{a}_i\cdot\mathbf{a}_j^* = 2\pi\delta_{ij}$ and there are $N_{\rm cell}$ of them in the BZ.[8,9,26] The inverse cluster transform is

$$X_{IJ} = \frac{1}{N_{\rm cell}} \sum_{\mathbf{K}_n\in{\rm BZ}}^{N_{\rm cell}} X(\mathbf{K}_n) e^{-i\mathbf{K}_n\cdot\mathbf{R}_{IJ}}. \tag{14}$$

X_{IJ} is translational invariance only if both (13) and (14) hold, implying that X_{IJ} is only dependent on the displacement between the cluster sites $\mathbf{R}_{IJ}$. Therefore, one could do the cluster transform in (13) based on any site in the cluster (translational invariance), leading to $N_{\rm cell}$ independent entries.

However, $J_{IJ}(\mathbf{k})$, known *a priori* from H in (1), is not translational invariant for a general cluster. The intercell Fourier transform in (11) results in the dependence on two indices, I and J, or, equivalently, I and $I-J$, making it site dependent. Considering nearest-neighbor (NN) interaction, a central site in a large (enough) cluster will not incur a phase factor (as all interactions are contained in the cluster) during the intercell Fourier transform, but a site at the perimeter of the cell has a phase factor via interaction with a site from an adjacent cell; hence, $J_{IJ}(\mathbf{k})$ is site dependent. To ensure translational invariance in the CG solution of $G_{IJ}(\mathbf{k})$ and $\tilde{\Sigma}_{IJ}$ within the cell, we multiply $J_{IJ}(\mathbf{k})$ by the phase $\exp(i\mathbf{k}\cdot\mathbf{R}_{IJ})$, as is done in the $\mathbf{r}$-space version of DCA (see Appendix in 7), resulting in the relation

$$G_{IJ}^{-1}(\mathbf{k}) = -\tilde{\Sigma}_{IJ} - \beta J_{IJ}(\mathbf{k}) e^{i\mathbf{k}\cdot\mathbf{R}_{IJ}}. \tag{15}$$

CG *in* $\mathbf{r}$ *-space*. From G_{IJ} a coarse-grained $\bar{G}_{IJ}$ is obtained via

$$\bar{G}_{IJ} = \frac{N_{\rm cell}}{N} \sum_{\mathbf{k}\in{\rm BZ'}} G_{IJ}(\mathbf{k}) e^{-i\mathbf{k}\cdot\mathbf{r}_{ij}}. \tag{16}$$

For $\mathbf{r}_{ij}=0$, when only sites from the same cell are of interest, the procedure is exactly analogous to that used in CDMFT or DCA, when (12) or (15) is coarse grained, respectively; the cell Brillouin zone, BZ', is $1/N_{\rm cell}$ of the lattice BZ. The $\mathbf{r}$-space formulation allows for the representation of any general ordered phases with multiple sublattices.[7]

CG *in* $\mathbf{k}$ *-space*. For cases with one sublattice, i.e., paramagnetic or ferromagnetic phases, the solution from DCA is diagonal in $\mathbf{k}$ space. Applying the cluster transformation,[8] shown in (13), to (15) yields

$$G(\mathbf{k}+\mathbf{K}_n) = [-\tilde{\Sigma}(\mathbf{K}_n) - \beta J(\mathbf{k}+\mathbf{K}_n)]^{-1}, \tag{17}$$

where $J(\mathbf{k}+\mathbf{K}_n)$ is equivalent to the lattice Fourier transform of J. The result, $G(\mathbf{k}+\mathbf{K}_n)$, is further coarse grained about $\mathbf{K}_n$ as

$$\bar{G}(\mathbf{K}_n) = \frac{N_{\rm cell}}{N} \sum_{\mathbf{k}\in\bar{\Delta}(\mathbf{K}_n)} G(\mathbf{k}+\mathbf{K}_n), \tag{18}$$

where the summation is over a zone $\bar{\Delta}(\mathbf{K})$ (a parallelogram in two dimensions and a parallelepiped in three dimensions), centered at $\mathbf{K}_n$, whose volume is $V_{\bar{\Delta}} = V_{\rm BZ}/N_{\rm cell}$; see Fig. 2. Equation (18) in integral form for an infinite lattice ($N\to\infty$) is

$$\bar{G}(\mathbf{K}_n) = \frac{1}{V_{\bar{\Delta}}} \int_{\mathbf{K}_n-\frac{1}{2}\Delta}^{\mathbf{K}_n+\frac{1}{2}\Delta} d\mathbf{k} G(\mathbf{k}+\mathbf{K}_n), \tag{19}$$

where the integral is over the same zone centered at $\mathbf{K}_n$ and defined by $\mathbf{K}_n \pm \frac{1}{2}\Delta$ with volume $V_{\bar{\Delta}}$. For DCA, $\mathbf{r}$-space CG $\bar{G}_{IJ}$ is related to $\bar{G}(\mathbf{K}_n)$ via a cluster transform,

$$\bar{G}_{IJ} = \frac{1}{N_{\rm cell}} \sum_{\mathbf{K}_n\in{\rm BZ}}^{N_{\rm cell}} \bar{G}(\mathbf{K}_n) e^{-i\mathbf{K}_n\cdot\mathbf{R}_{IJ}}. \tag{20}$$

B. Thermodynamic consistency

Without loss of generality, Ω in (8) can be written in terms of a functional $\Phi[G]$ (in many-electron physics, it would be the Baym-Kadanoff functional[27]):

$$\Omega[G] = -k_B T(\Phi[G] + {\rm Tr}\ln G - {\rm Tr}(\Sigma G)). \tag{21}$$

As in (9), for $\Omega[G]$ to be variational, i.e., $\delta\Omega/\delta G = 0$, it is necessary that

$$\frac{\delta\Phi[G]}{\delta G} = \Sigma = G_0^{-1} - G^{-1}, \tag{22}$$

where G and G_0 are the full lattice and bare Green's functions, respectively. In quantum cluster theories, $\Phi[\bar{G}]$ is used in place of $\Phi[G]$, and, as such, a coarse-grained Dyson's equation is satisfied[8] if (22) uses $\Sigma\to\tilde{\Sigma}$ and $G\to\bar{G}$. Importantly, when $\tilde{\Sigma}$ and $\bar{G}$ are utilized in a proper cluster version of Ω, i.e., $\Phi[\bar{G}]$ is used in (21) and the CG version of (22) is required, the estimated grand potential is still variational with respect to G,[8] and they yield the necessary relation between the lattice self-energy and that of the cell (10).

C. Self-consistent embedded cluster solver

A connection has to be made between the lattice variables (divided into cells) and the cluster variables evaluated via the cluster $\hat{Z}[A]$ [see (A7) and (A6)]:

$$\hat{G}_{ij} = \frac{{\rm Tr}_{\sigma\in c}\sigma_i\sigma_j e^{\hat{H}(\mathcal{G}^{-1},\beta m J,\sigma)}}{{\rm Tr}_{\sigma\in c} e^{\hat{H}(\mathcal{G}^{-1},\beta m J,\sigma)}}, \tag{23}$$

where the trace is over sites within the cluster and $\hat{Z}[A=0]$ is the denominator. The cluster $\hat{H}$ consists of "dressed" effective intracluster-site interactions

$$\mathcal{G}^{-1} = \bar{G}^{-1} + \tilde{\Sigma}, \tag{24}$$

and the mean field mJ for coupling to sites exterior to the cluster.

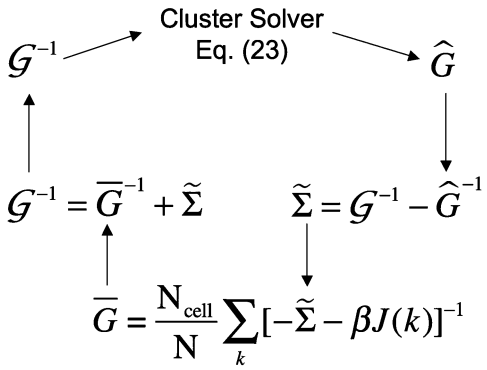

FIG. 3. Self-consistency loop (see Sec. III C for details) for solving the CMFT problem in the case of $N_{\rm cell} = N_c$.

For comparison with DCA and CDMFT (see Fig. 6 in Ref. 8), Fig. 3 shows a self-consistency loop for the case when $N_{\rm cell} = N_c$. A chosen CG method [Eq. (16) for **r** space or (20) for **k** space] is used in conjunction with the cluster solver in (23). Starting from an initial guess for $\tilde{\Sigma}$, the following steps should be followed.

(1) $\bar{G}$ is evaluated from a CG equation.

(2) Effective interaction $\mathcal{G}^{-1}$ is calculated for use in cluster solver (23).

(3) $\hat{G}$ from (23) is used to obtain a new $\tilde{\Sigma}$.

(4) Repeat steps (1)–(3) until $\tilde{\Sigma}$ converges, upon which

$$\hat{\Sigma} = \tilde{\Sigma}, \quad \hat{G} = \bar{G}. \tag{25}$$

Importantly, this outcome is not the case in the CMFT of Tokar[15] [from which (23) was first derived], where CG was not applied and the Dyson's equation (3) was used directly via a lattice Fourier transform in conjunction with (23). To connect to that work, we must consider $N_{\rm cell} > N_{\rm c}$, in which only some of the components in $\bar{G}$ and $\tilde{\Sigma}$ are projected out for use in the cluster solver. For clarity, we discuss the result of this in Sec. IV D.

D. Solving for cluster $\hat{G}$ and $\hat{\Sigma}$

To obtain the cluster $\hat{F}$, $\hat{\Sigma}$ and $\hat{G}$ have to be evaluated. Although one can utilize the iterative scheme in Fig. 3, we solved the appropriate equations simultaneously using the fsolve function in MATLAB.[28] Assuming only that the cluster matrices are symmetric, the number of independent elements in $\hat{\Sigma}$ is

$$M_v = N_{\rm c} + \frac{N_{\rm c}(N_{\rm c}-1)}{2}. \tag{26}$$

Hence, with both $\hat{\Sigma}$ and $\hat{G}$, we have $2M_v$ independent variables. From the cluster partition function $\hat{Z}[A]$, there are $N_{\rm c}$ equations for m_i (or, equivalently, $\hat{G}_{ii}$) and $N_{\rm c}(N_{\rm c}-1)/2$ equations for $\hat{G}_{i\neq j}$ [see (A7)], giving us M_v independent self-consistent equations.

On the other hand, from the cell partitioning of the Dyson's relation, we use M_v equations from (16) that relates $\bar{G}$ to the lattice self-energy $\tilde{\Sigma}$. Combining with those from the cluster approximation, we have $2M_v$ independent equations to solve for the $2M_v$ unknown cluster variables, $\hat{\Sigma}$ and $\hat{G}$. The lattice variables are dependent variables because their exact mapping to the cluster variables is given by (25).

Even though our code had not been fully optimized, we find that the method is especially fast when N_c is small ($N_c < 10$). Use of DCA CG further reduces M_v via the appropriate treatment of translational invariance, where cluster sites belonging to the same sublattice are made equivalent. For the FM Ising model, $M_v = N_{\rm c}$, speeding up calculations. At second-order FM T_c, the uniform susceptibility $\beta G(\mathbf{K}_n = 0, \mathbf{k} = 0)$ diverges, i.e., from (17),

$$\tilde{\Sigma}(\mathbf{K}_n = 0) + \beta_c J(0) = 0, \tag{27}$$

as an extra constraint for determining β_c at criticality.

E. The cluster free energy

With $\hat{G}$ and $\hat{\Sigma}$ obtained via DCA CG, we evaluate the cluster $\hat{F}$ required for constructing boundaries between different phases. Via the cluster partition function[15] in (A6) and the definition of pair-correlation energy (5), we are able to express the cluster free energy $\hat{F}$ as

$$\hat{F} = E_1 + \hat{E}_2 - T\sum_{\rm c}\hat{S} - \frac{k_B T}{2}\left[\ln\det G - \sum_{\rm c}\ln\det\hat{G}\right]. \tag{28}$$

Here c denotes independent clusters in the lattice, and $\hat{S}$ is the cluster entropy, which reduces to point entropy for $N_{\rm c} = 1$. The last term gives the Gaussian part of the pair correlations in the lattice relative to those in the cluster (see the Appendix), where, for $N_{\rm c} = \infty$, the free energy is exact and the term in brackets is zero. Of course, (28), which is familiar in classical cluster theories, can be rewritten as (21), which is familiar in correlated-electron theories, using (5) and (8) with $\hat{F} = \hat{\Omega}[0]$.

IV. RESULTS AND DISCUSSION

We apply the cluster methods from various cluster-lattice Fourier transforms to the FM and AFM Ising model (with NN interactions only) on one-dimensional (1D) and three-dimensional (3D) (fcc) lattices. We discuss results from the DCA (i.e., $N_{\rm cell} = N_{\rm c}$), giving a one-to-one mapping of the cluster variables to the lattice cell variables. We also discuss results with the $N_{\rm cell} > N_{\rm c}$ scheme, with $N_{\rm cell} = \infty$ being the NCG version, which do not exhibit the one-to-one mapping and do not preserve translational invariance but do conserve the sum rules and provide accurate estimates of thermodynamics. We first show the improvement for the estimation of T_c for $N_{\rm c} = 1$. Then, we discuss DCA results for multisite clusters in various lattices, including finite-size scaling of T_c versus $N_{\rm c}$ for the fcc FM and AFM (including tricritical points) that yield exact values at $N_{\rm c} \to \infty$. Last, we compare results obtained by the DCA and NCG scheme. The NCG version converges thermodynamic quantities more rapidly versus $N_{\rm c}$ using significantly less computational time.

A. Weiss single-site MFT

The consistency between $\hat{G}$ estimated from $\hat{Z}[A]$ and G obtained from Dyson's equation is ignored in textbook MFTs (e.g., Weiss, Bethe,[29] quasichemical method[30]), where $\hat{Z}[A]$ is formulated without proper treatment of Σ; G_{ii} evaluated via (7) violates (2b). In the Weiss model,[16] spin correlations

are completely neglected, as in a disordered phase. With $c_i^{\pm} \equiv (1 \pm m_i)/2$, the free energy is obtained by including the point entropy S_1, i.e.,

$$F_1 = E_1 - T\left[- k_B \sum_i (c_i^+ \ln c_i^+ + c_i^- \ln c_i^-)\right]. \quad (29)$$

The functional F_1 is minimized with respect to m_i or via (9) to obtain m_i from the coupled set of equations

$$m_i = \tanh\left[\beta \sum_j J_{ij} m_j + \beta h\right] . \quad (30)$$

Equation (30) gives the Weiss result[16,17] and is frequently used to illustrate phase transitions. However, it gives poor quantitative estimates of T_c and phase boundary topology. For the zero-field case, the Weiss model incorrectly predicts FM ordering at $T_c = zJ$ (instead of $T_c = 0$) for the 1D lattice where $z = 2$. The Weiss model is only correct[31] in the limit of infinite dimensions or at finite dimension for infinite-ranged J. Estimates are improved with MFTs that extend beyond single site, such as the Bethe[29] and quasichemical methods.[30] For example, the Bethe approximation correctly predicts the 1D FM T_c to be zero[32] and improves estimates of T_c at higher dimensions. However, the inaccuracies are exacerbated when describing transitions for frustrated lattices. For AFM on an fcc lattice, the Weiss model fails to predict even qualitatively the correct topology given by MC; see Fig. 1. Although the quasichemical methods somewhat improve the topology, the boundary approaches $T = 0$ incorrectly.[33,34]

In the Krivoglaz, Clapp, and Moss (KCM) approximation for the self-energy[35,36] of the Weiss model

$$\Sigma_{ij}^{\mathrm{KCM}} = -\delta_{ij}\left(1 - m_i^2\right)^{-1} . \quad (31)$$

When (31) is substituted into (7), it does not satisfy the sum rule[24,25] in (2b); i.e., the Weiss model simply solves the approximate partition function via (30) regardless of the value of lattice G_{ii} from (7). Thus, to satisfy the sum rule, Σ_{ii} must be "adjusted" such that the resulting value of G_{ii} in (7) coincides with that obtained from (9) for an approximated $Z[A]$, which satisfies (2b) by construction, as is done by Onsager's cavity field theory[18–20] and Brout's spherical model.[21,22,37] Results for G via (3) can be improved progressively as the approximation for Σ becomes more sophisticated, e.g., the gamma expansion method (GEM)[14] that includes off-diagonal entries or the Ring approximation that includes infinite sums of subsets of a diagrammatic expansion.[38] In our case, Σ_{ii} is adjusted such that G_{ii} evaluated via (7) coincides with $\hat{G}_{ii}$ from the cluster partition function (23), as explained in Sec. III C for $N_{\mathrm{cell}} = N_c = 1$.

B. Accurate single-site CG DCA theory

The estimate of phase transitions for the single-site case is improved via a CG DCA approach. At $N_c = 1$, applying (9) to the cluster $\hat{Z}[A]$[15] [see (A7)], we obtain

$$m_i = \tanh\left[\left(\hat{G}_{ii}^{-1} + \Sigma_{ii}\right)m_i + \beta \sum_j J_{ij} m_j + \beta h\right] \quad (32)$$

and $\hat{G}_{ii} = 1 - m_i^2$, which has the obvious on-site correction from the sum rule [cf. (30)]. We can also derive (32) by minimizing (28) with respect to m_i or from (1), assuming that J_{ii} is nonzero such that (3) is obeyed. This result was also found by Tokar and Tsatskis[39] by assuming coherent potential approximation (CPA)-like embedding and ignoring boundary effects. Thus, for $N_c = 1$, $\hat{F}$ in (28) simplifies to

$$E_2 = \frac{k_B T}{2} \sum_i (1 + \hat{G}_{ii}\hat{\Sigma}_{ii}) \quad (33a)$$

$$\sum_c \ln\det \hat{G} = \sum_i \ln \hat{G}_{ii} \quad (33b)$$

$$\ln\det G = -\frac{N}{V_{\mathrm{BZ}}} \int_{\mathrm{BZ}} d\mathbf{k} \ln(-\Sigma_{ii} - \beta J(\mathbf{k})) \quad (33c)$$

and $\sum_i \hat{S}$ becomes the point entropy S_1. Note that (33c) is valid only for single sublattice phases.

To relate correctly the cluster and lattice variables, the $N_c = 1$ DCA sets $\tilde{\Sigma}_{ii} = \hat{\Sigma}_{ii}$, and (20) simplifies to (7), i.e., $\hat{G}_{ii} = G_{ii}$, satisfying (2b). Together with (32), we have a coupled set of equations for estimating thermodynamic state variables for the Ising model for a given T and h, utilizing (28) with (33) to obtain free energies.

1. *First-order AFM ($J = -1$) on a fcc lattice*

The free energies of the $L1_0$- and $L1_2$-ordered ground states are compared with the high-T disordered $A1$ phase, allowing construction of the phase diagram. In Fig. 1, the T-h phase diagram for the fcc Ising model obtained via DCA $N_c = 1$ [i.e., (2b), (7) and (32)] is compared with that of the Weiss model[17] and MC (exact). The DCA $N_c = 1$ gives a good estimate of the topology from MC, although the tricritical-point temperature is higher compared to MC. Nonetheless, the results are a huge improvement over the the Weiss model, in which the phase boundaries are not even qualitatively close to the exact topology. We emphasize that this results from including self-correlation to the single-site Weiss magnetization, as shown in (32).

2. *Second-order FM ($J = 1$) at $h = 0$*

Above T_c, (32) is automatically satisfied by $m_i = 0$ for all sites, i.e., the paramagnetic state. For a second-order transition, the uniform susceptibility $\beta G(\mathbf{k} = 0)$ diverges at T_c.[32] The denominator of the integrand in (7) is thus zero at $\mathbf{k} = 0$, i.e., $\Sigma_{ii} = -\beta_c J(\mathbf{k} = 0)$, giving

$$G_{ii} = \frac{1}{\Omega \beta_c J(0)} \int \frac{d\mathbf{k}}{1 - J(\mathbf{k})/J(0)}. \quad (34)$$

With $G_{ii} = 1$ (given $m_i = 0$), only β_c must be determined. Although the integrand contains a singularity at $\mathbf{k} = 0$, the integral (a lattice Green's function[40]) is convergent[41] for cubic lattices, and the numerical values are given in Ref. 37. We have obtained them via numerical integration using MATLAB.[28] In the 1D case, the integral is divergent, requiring $\beta_c \to \infty$ for G_{ii} to be finite, so the cluster method yields the correct result of $T_c = 0$ in one dimension. For the FM fcc case, T_c is only 8.9% lower than the exact result, a significant improvement over the Weiss model (22.5% higher), while retaining the mathematical

simplicity. Thus, the DCA $N_c = 1$ result is equivalent to that found by Tokar.[15]

C. Multisite cluster CG theory

1. FM on a 1D lattice

For the 1D chain, we now study the effect of obeying the sum rule in (2b) for general cluster sizes. The uniform lattice susceptibilities (ULS), $\beta G(\mathbf{K}_n = 0, \mathbf{k} = 0)$, at $J = 1$ and $T = 1.2$, obtained by the DCA and Weiss-like MFT are compared in Fig. 4. The isolated (finite-size) cluster approximation [see (13) in Ref. 8] only takes into account interactions between atoms in an isolated, finite-size cluster whose partition function is calculated via the transfer-matrix method. The cluster MF approximation [see (14) in Ref. 8] further adds in a mean-field contribution to the cluster, with the Weiss model being the single-site cluster MF. Neither isolated cluster nor cluster MF approximations require the lattice G to satisfy (2b).

Improvements in accuracy are apparent, especially at low cluster size ($N_c < 8$). At fixed N_c cluster size, the inclusion of MFT corrections improves the estimate of ULS (cf., isolated cluster and cluster MF methods) and is further improved upon by taking into account the intensity sum rule (cf., cluster MF and DCA). In addition, while DCA MFT shows a monotonic convergence (from below) to the exact value versus N_c, the cluster MF estimate overshoots the exact value at $N_c = 9$, resulting in a temporary loss in accuracy.

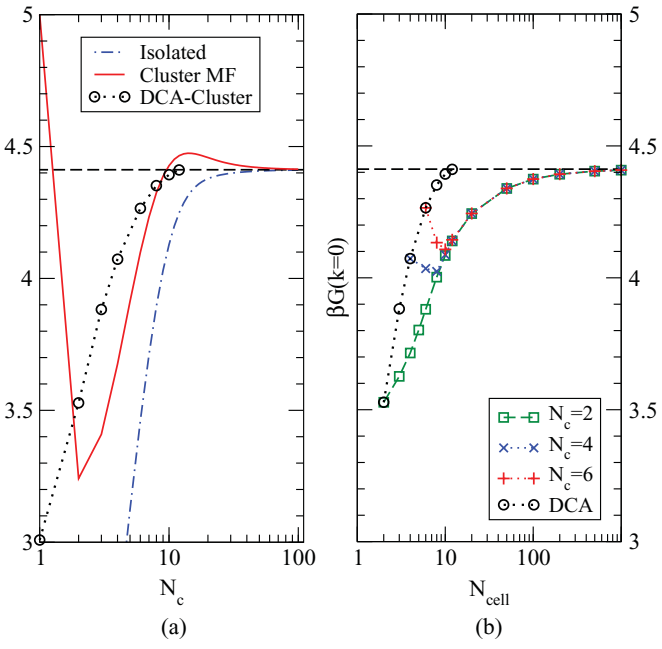

FIG. 4. (Color online) The 1D FM uniform lattice susceptibility for $J = 1$ and at $T = 1.2$ vs (a) N_c and (b) N_{cell}, with the exact value at $N_c = \infty$ given by the horizontal (dashed) line. (a) The CG DCA ($N_{\text{cell}} = N_c$) results are compared with those from the isolated cluster and cluster MF.[8] (b) Our CMFT for $N_{\text{cell}} > N_c$ ULS vs N_{cell} is shown for N_c of 2, 4, and 6, yielding the exact result at $N_{\text{cell}} \approx 1000$; all results collapse on a single curve for $N_{\text{cell}} \gtrsim 2N_c$. CG DCA results are shown (circles joined by dotted line) for comparison.

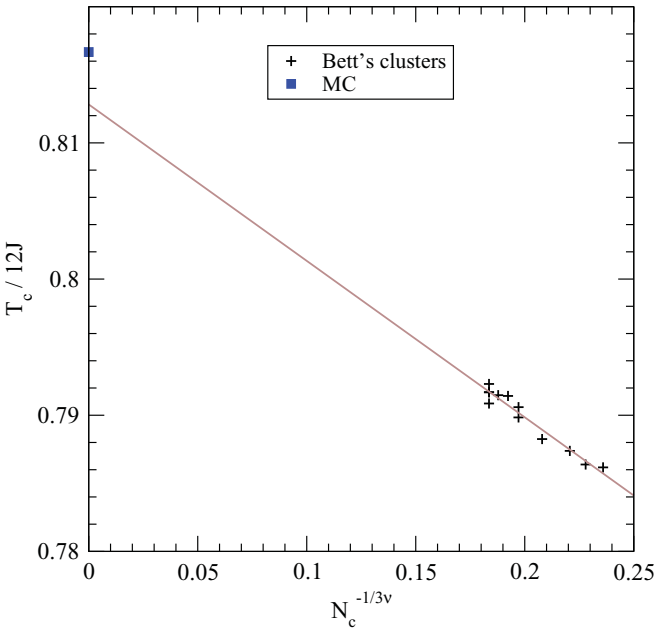

FIG. 5. (Color online) Finite-size scaling (35) for the fcc FM Ising model with $\nu = 0.625$. The line is a linear fit to T_c^{DCA} using Bett's clusters (pluses) for $15 \leqslant N_c \leqslant 24$. $T_c/12J = 0.813$ for $N_c = \infty$ compared to 0.8167 from MC (square).

2. FM on a fcc lattice with finite-size scaling

The DCA MFT exhibits finite-size scaling for T_c versus N_c, as we show in Fig. 5 using Bett's clusters[13] with $15 \leqslant N_c \leqslant 24$ values are tabulated in Table II. T_c are plotted along with the finite-size scaling law,

$$\left\| T_c^{\text{DCA}} - T_c^{\text{exact}} \right\|^{-\nu} \sim L = N_c^{1/3}, \tag{35}$$

where $0.625 \lesssim \nu \lesssim 0.63$ for the 3D Ising universality class.[42,43] We use $\nu = 0.625$, although our findings are not affected by other choices in the range. The scaling curve is extrapolated to $N_c = \infty$, giving a value of $T_c/12J = 0.813$, close to the MC exact result of 0.8167.

3. AFM on a fcc lattice with finite-size scaling

For the AFM case, multiple sublattices are used to describe the $L1_0$ and $L1_2$ states, which exhibit frustration. As a result, the real-space CG is used; see (15) and (16). In Fig. 6, phase boundaries from single-site DCA (already shown in Fig. 1) are compared with those from DCA and CDMFT multisite clusters with $N_c = 4$ or 16 and exact results from MC. Because the single-site estimates of T_c near stoichiometry are already excellent, the improvement with increased cluster size is minor at $h/|J| = 0$ and $h/|J| \simeq 7.7$, where only two phases compete. However, at the tricrtical point T_t, where the three phases ($L1_0$, $L1_2$, and $A1$) coexist, there is a significant improvement. As N_c increases, T_t progressively decreases and approaches the MC value of $T_t/|J| \simeq 1$.

A fit to the finite-size scaling (35) for T_t using $N_c = 4$ and 16 DCA is shown in Fig. 7. Although, ideally, one would prefer to include larger clusters for scaling, the calculations are computationally expensive for $N_c > 4$ clusters, especially with the multiple sublattices involved, in which case exact MC simulations must be preferred. Nevertheless, the extrapolated

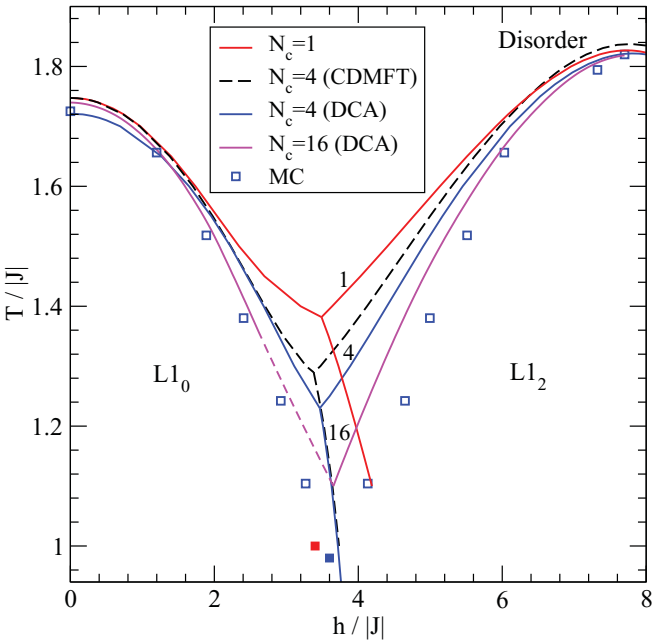

FIG. 6. (Color online) T-h boundaries for fcc AFM, showing $A1$, $L1_0$, and $L1_2$ phases. CG boundaries for DCA-like $N_c = N_{cell} = 1$, 4, and 16 are labeled, along with DMFT-like boundaries with $N_c = 4$. MC results are marked by squares (unfilled are ours, and filled are tricritical points from Refs. 44 and 45). For $N_c = 16$ DCA, the $A1$-$L1_0$ boundary below $T/|J| = 1.35$ is extrapolated due to poor numerical convergence. The tricritical point approaches the MC result as N_c increases.

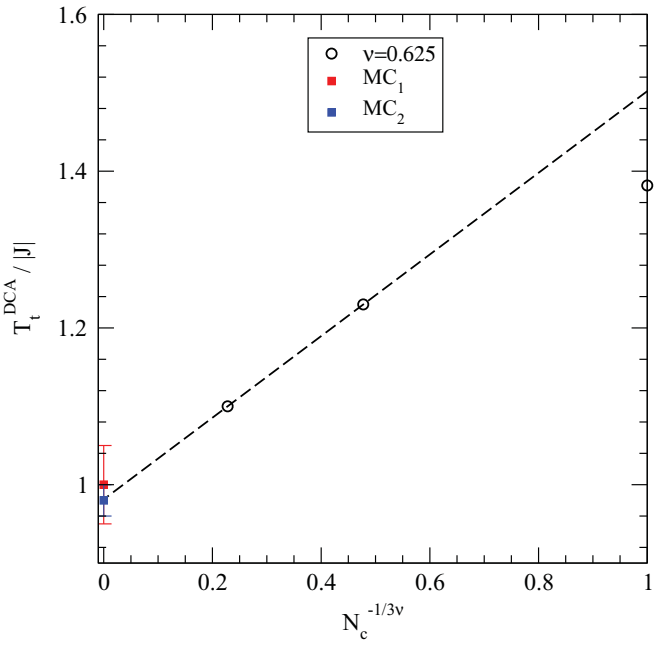

FIG. 7. (Color online) Finite-size scaling (35) for tricritical point T_t in Fig. 6 for fcc AFM for $N_c = 1$, 4, and 16 DCA (open circles). The dashed line is a fit to $N_{cell} = N_c = 4$ and 16. The T_t at $N_c = \infty$ is within the error bars of MC data from Refs. 44 (red top square) and 45 (blue bottom square).

result at $N_c = \infty$ ($T_t/|J| = 0.98$) is within the error bars of MC data.

D. NCG versus CG CMFT

We now discuss the case of $N_{cell} > N_c$; i.e., $\tilde{\Sigma}$ and $\hat{\Sigma}$ are of different sizes, where

$$\tilde{\Sigma}_{\tilde{I}\tilde{J}} = \begin{cases} \hat{\Sigma}_{IJ} & \text{if } |\mathbf{R}_{\tilde{I}\tilde{J}}| = |\mathbf{R}_{IJ}| \\ 0 & \text{otherwise.} \end{cases} \tag{36}$$

The terms belonging to the same NN distance are equal. For example, the unique NN term $\hat{\Sigma}$ (a 2×2 matrix) is assigned to all NN entries in $\tilde{\Sigma}$ with all entries beyond NN set to zero. For $N_{cell} > N_c$, only some of the components in $\bar{G}$ and $\tilde{\Sigma}$ are projected out for use in the cluster solver, i.e.,

$$\hat{\Sigma} = P_c \tilde{\Sigma} P_c', \quad \hat{G} = P_c \bar{G} P_c', \tag{37}$$

where P_c is a $N_c \times N_{cell}$ projection matrix. So there exists a one-to-many relation in going from $\hat{\Sigma}$ to $\tilde{\Sigma}$. Tokar's results corresponds to $N_{cell} \to \infty$ and N_c remains finite; thus, $\tilde{\Sigma}$ is sparse and has nonzero components up to the longest pair in $\hat{\Sigma}$. The proper boundary conditions and the relation between cluster and lattice variable are missing in the original theory, which are restored only with proper CG with $N_{cell} = N_c$.

We note that the consistency relation is enforced for sites belonging to the same projected cluster space, which does not preclude the calculation of G_{IJ} between sites of different clusters via (16) with nonzero $\mathbf{r}_{ij}$. Importantly, we have shown how the cluster variables from $\hat{Z}[A]$ are related to the CG lattice variables, allowing us to solve a system of coupled equations.

To further illustrate this point, we consider the 1D lattice using a $N_c = 3$ cluster; see Fig. 8 (top row). In the FM case, the cluster self-energy is given by

$$\hat{\Sigma} = \begin{bmatrix} s_{11} & s_{12} & s_{13} \\ s_{12} & s_{11} & s_{12} \\ s_{13} & s_{12} & s_{11} \end{bmatrix}, \tag{38}$$

where the diagonal terms are equal and the off-diagonal terms are labeled by the distance between sites in the cluster; s_{12} for NN and s_{13} for the next NN (NNN). The assignment to the lattice $\tilde{\Sigma}$ is made via (36) and is illustrated in Fig. 8 for $N_{cell} = 3$, 4, and ∞. For the DCA, the lattice self-energy is partitioned into cells such that $\bar{\Sigma} = \hat{\Sigma}$, and $\tilde{\Sigma}$ is translational invariant, so $s_{12} = s_{13}$. This is possible by virtue of (15), where each term satisfies the cluster transformation in (13) and its inverse (14). The periodicity of the cell requires that the NNN term between sites 1 and 3 in the same cell (see Fig. 8, top row) be the same as the NN term between site 1 (same cell) and site 3 in the left adjacent cell.

At $N_c = 3$ still, Fig. 8 illustrates the relation in (36) for $N_{cell} = 4$ (middle row) and $N_{cell} \to \infty$ (bottom row), showing that $\hat{\Sigma}$ no longer has a one-to-one mapping to $\tilde{\Sigma}$. In the case of $N_{cell} = 4$, from (36) and (38), we have

$$\tilde{\Sigma} = \begin{bmatrix} s_{11} & s_{12} & s_{13} & 0 \\ s_{12} & s_{11} & s_{12} & s_{13} \\ s_{13} & s_{12} & s_{11} & s_{12} \\ 0 & s_{13} & s_{12} & s_{11} \end{bmatrix}. \tag{39}$$

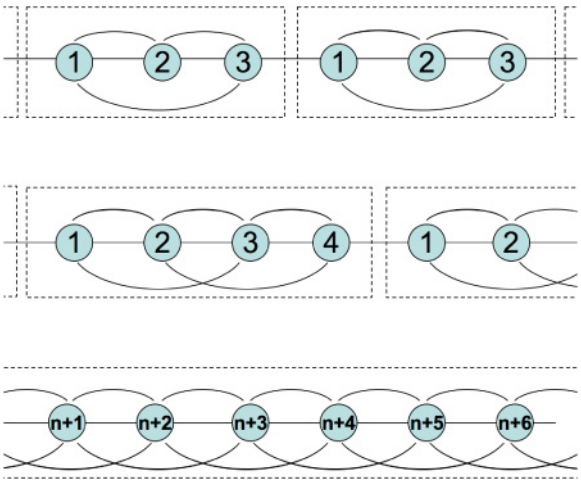

FIG. 8. (Color online) Partitioning of the lattice $\tilde{\Sigma}$ into cells with N_{cell} equal to (top) 3, (middle) 4, and (bottom) ∞. For $N_c = 3$, the top (bottom) row corresponds to the CG (NCG) scheme. For each row, the upper and lower arrays of connectors represent the NN and NNN self-energy terms, respectively. Connectors are missing between cells, except for the $N_{cell} = \infty$ case (bottom).

$\tilde{\Sigma}$ is thus site dependent and, therefore, not translational invariant. For $N_{cell} \to \infty$, each term (s_{11}, s_{12}, and s_{13}) is periodically repeated throughout the lattice.

Once $\tilde{\Sigma}$ is assigned, one can follow the steps laid out in Sec. III A to obtain the CG $\bar{G}$. Using the **k**-space formulation for illustration, with the non-coarse-graining method, where $N_{cell} = N \to \infty$, Eq. (19) is reduced to

$$\bar{G}(\mathbf{K}_n) = \lim_{V_{\tilde{\Delta}} \to 0} \frac{1}{V_{\tilde{\Delta}}} \int_{\mathbf{K}_n - \frac{1}{2}\Delta}^{\mathbf{K}_n + \frac{1}{2}\Delta} d\mathbf{k} G(\mathbf{k} + \mathbf{K}_n) = \frac{G(\mathbf{K}_n) \times V_{\tilde{\Delta}}}{V_{\tilde{\Delta}}} = G(\mathbf{K}_n). \quad (40)$$

Substituting into Eq. (20), we have

$$\bar{G}_{IJ} = \lim_{N_{cell} \to \infty} \frac{1}{N_{cell}} \sum_{\mathbf{K_n} \in \mathrm{BZ}}^{N_{cell}} G(\mathbf{K}_n) e^{-i\mathbf{K}_n \cdot \mathbf{R}_{IJ}} = \int_{\mathrm{BZ}} \frac{d\mathbf{K}}{V_{\mathrm{BZ}}} G(\mathbf{K}) e^{-i\mathbf{K}\cdot\mathbf{R}_{IJ}}, \quad (41)$$

$$\bar{G}_{IJ} = \int_{\mathrm{BZ}} \frac{d\mathbf{K}}{V_{\mathrm{BZ}}} [-\tilde{\Sigma}(\mathbf{K}) - \beta J(\mathbf{K})]^{-1} e^{-i\mathbf{K}\cdot\mathbf{R}_{IJ}}. \quad (42)$$

$\bar{G}$ is thus obtained via a Fourier transform, i.e., no coarse graining is used. One obtains the same conclusion using the **r**-space CG formalism in (16) because BZ'$\to$ 0 and the summation is over a point at $\mathbf{k} = 0$. This result was used by Tokar[15] by ignoring the difference between cluster-lattice transforms of matrices $\boldsymbol{J}$ and $\boldsymbol{\Sigma}$ due to phase factors at the cell boundaries. Again, this relation is the NCG scheme anticipated in the introduction.

1. FM in the 1D lattice

To investigate the effect of varying N_{cell}, the ULS of the 1D lattice (at $J = 1$ and $T = 1.2$) is shown in Fig. 4(b) at fixed $N_c = 2$, 4, and 6 (squares, crosses, and pluses, respectively), with comparison to DCA ($N_{cell} = N_c$ with $2 \leqslant N_c \leqslant 12$, given by circles). Except for an initial loss in accuracy (due to loss of translational invariance), the ULS converges monotonically to the exact value and converges at $N_{cell} \approx 1000$. Convergence is reached by the DCA at $N_c \approx 12$, but at the cost of solving for many more degrees of freedom.

TABLE I. Relative CPU time for 1D Ising FM versus N_{cell} for the $N_{cell} = N_c$ DCA and at a fixed cluster size of $N_c = 2$ with $N_{cell} \geqslant N_c$. For a given row, both methods yield the same value of $\beta G(\mathbf{k} = 0)$; see Fig. 4(b).

$N_c = N_{cell}$		$N_c = 2$
N_{cell}	CPU Time	N_{cell}
2	1.0 1.0	2
3	1.2 0.3	6
4	2.1 0.4	10
6	7.0 0.7	26
8	28 1.4	58
10	148 4.7	200
12	957 23	1000

In addition, we compare the CPU time for the DCA and the NCG methods with $N_{cell} > N_c$ at fixed values of ULS, i.e., at a fixed level of accuracy, as shown in Table I. For example, from Fig. 4(b), the ULS for DCA at $N_c = 6$ has the same level of accuracy as that of $N_c = 2$ with $N_{cell} = 26$. As seen in Table I the CPU time is much less for NCG because the number of independent cluster variables remains at $2N_c$ regardless of N_{cell}. The relationship can also be explained from another perspective. For $N_c = 6$ DCA, we must solve for 12 variables; however, one could trade computation time for accuracy by keeping terms only up to the NN (neglecting the rest), effectively doing a $N_c = 2$ calculation with $N_{cell} = 6$.

2. FM on the fcc lattice

For the FM transition, T_c on the fcc lattice is also compared, and the results are tabulated in Table II, together with exact T_c from MC and series expansion. As shown, at $N_c = 1$ the cluster method (−8.9% deviation) already gives a huge improvement over the single-site Weiss estimation (23% deviation). The DCA and the NCG methods are equivalent at $N_c = 1$. For the DCA, we observe that the T_c progressively approaches the exact value from below as N_c increases. This is in contrast to NCG, where T_c^{exact} approaches monotonically from above and is more rapidly convergent than DCA versus N_c.

3. AFM on the fcc lattice

We applied the NCG method to the fcc AFM case with multisite clusters. Although the free energy of the disordered system can be obtained for a given T and h, we failed to get converged multisublattice ordered solutions for $\hat{\Sigma}$ and $\hat{G}$. The free energies of ordered phases could not be obtained, and thus, transitions could not be predicted. In the NCG scheme, $N_{cell} = \infty$, while a finite N_c cluster is used for the configurational average; hence, $\hat{\Sigma}$ is evaluated only for pairs within the (smaller) cluster, i.e., entries are nonzero in the (larger) cell only up to a certain range. However, from the perspective of DCA where $N_{cell} = N_c$, all values of $\hat{\Sigma}$ are potentially finite. Although the values of Σ_{ij} decrease rapidly

TABLE II. Curie temperature ($T_c/12J$) for various CMFT and cluster sizes on a fcc lattice. Percentage deviation (% Dev.) from a series expansion (considered exact[46]) and finite-sized scaled MC results are given. CG results (equivalent to DCA) from optimal Bett's clusters (used in Fig. 5) are labeled as in Ref. 13. NCG results exhibit faster convergence and agree with that from Ref. 15. CG and NCG are equivalent at $N_c = 1$.

N_c	Label	$T_c/12J$	% Dev.	Method
1		1.0000	+22.5	Weiss
1		0.7437	−8.9	NCG
2		0.8344	+2.2	NCG
3		0.8264	+1.2	NCG
4		0.8200	+0.5	NCG
1		0.7437	−8.9	CG
4		0.7729	−5.3	CG
15	B	0.7862	−3.7	CG
16	A	0.7864	−3.7	CG
17	A	0.7874	−3.5	CG
19	A	0.7883	−3.4	CG
21	A	0.7898	−3.2	CG
21	E	0.7906	−3.1	CG
22	B	0.7914	−3.0	CG
23	A	0.7915	−3.0	CG
24	C	0.7917	−3.0	CG
24	D	0.7909	−3.1	CG
24	F	0.7923	−2.9	CG
24	K	0.7917	−3.0	CG
∞		0.8167	+0.06	MC
∞		0.8162	–	Series expansion

with shell distance for the disordered phase[47] (also observed in our work), this is not the case for the ordered system. For example, Fig. 9 shows the converged values of $\tilde{\Sigma}$ for various values of T at $N_c = 4$ at $h = 0$. The magnitude of the NN term is smaller than the on-site term, and the magnitudes of the disordered phase terms are correspondingly smaller than that for the ordered $L1_0$ phase. In particular, the NN term for different sublattices in $L1_0$ is 4 times larger than that of the disordered NN term. More investigation is needed to understand the convergence issues for the solution of the NCG method for general symmetry-broken ordered states.

V. CONCLUSION

From a cluster-lattice, coarse-graining (CG) transform with $N_{\text{cell}} \geqslant N_c$, we derived a set of cluster MFTs for the Ising Hamiltonian involving the lattice Green's function (static pair correlations) and self-energy. For $N_c = N_{\text{cell}}$ we recover the equivalent approximations used in the DCA and CDMFT. In the DCA approach, the lattice partition function $Z[A]$ is simplified by considering only configurations within an N_c-site cluster $\hat{Z}[A]$ such that the cluster pair correlation $\hat{G}$ is consistent with the CG lattice $\bar{G}$ from Dyson's equation (3). As a result, $\bar{G}$ inherently obeys the lattice sum rules in (2) for $i, j \in$ cluster, which is violated in most other MFTs. In addition, using the DCA, we modified the Ising model cluster solver from Tokar[15] and obtained a closed-form expression for the cluster grand potential that maintains thermodynamic

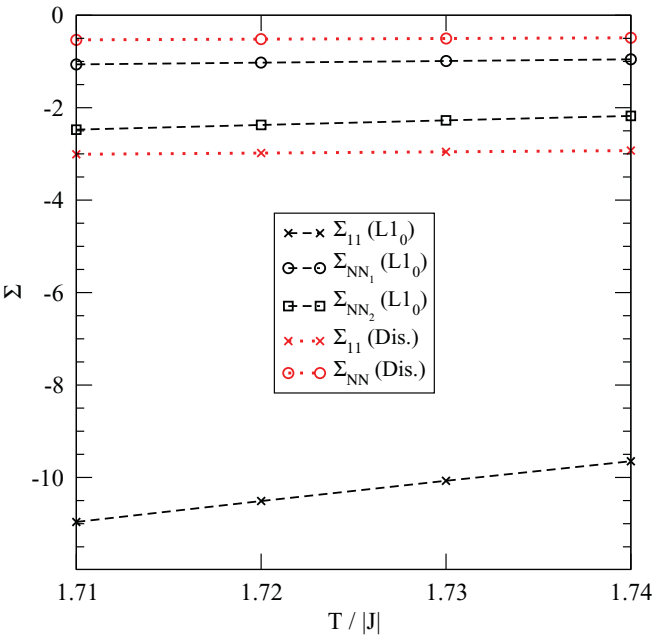

FIG. 9. (Color online) Coarse-grained Σ values versus T at $h = 0$ for $N_c = 4$ DCA (four-atom fcc cube) for $L1_0$ (dashed lines) and $A1$ (dotted lines) phases. Σ_{11} refers to on-site self-energy, while Σ_{NN} refers to the off-diagonal nearest neighbor. $L1_0$ contains two sublattices, where Σ_{NN_1} (Σ_{NN_2}) is the NN term between the same (different) sublattices.

consistency. The DCA formulation can be done in **r** space or **k** space and retains proper translational invariance and is, therefore, applicable to general clusters.

We applied this CG cluster MFT to the Ising model to predict phase transitions, for both T_c and T-h boundary topology. For general clusters, we studied the 1D FM case and both FM and AFM cases on a fcc lattice. The CG cluster MFT predicts T_c and phase boundaries approaching that of Monte Carlo, as illustrated for FM T_c and the AFM tricritical-point T_t versus N_c, including via finite-size scaling. Already at $N_c = 1$ for the AFM case, the predicted T_c are quantitative and topologically correct versus external field h; basically, the $N_c = 1$ case recovers the conservation of particle number forced within Onsager and Brout theories but has an improved, but equally simple, description of free energies for both first- and second-order phase transitions.

We extended these concepts to a NCG variant with $N_{\text{cell}} \gg N_c$, $N_{\text{cell}} \to \infty$, and showed that it was accurate and more computationally efficient for FM cases but does not guarantee translational invariance of general clusters for AFM ordering. This limiting case becomes equivalent to a MFT suggested by Tokar,[15] using ideas of the CPA that ignored cluster boundary conditions. For FM, the NCG variant requires a smaller N_c and, hence, much shorter computation time to achieve the accuracy from the DCA using larger clusters. The NCG method may be useful for larger quantum cluster calculations.

We are extending these concepts to multibody cluster expansions by expanding multibody correlations as cumulants, retaining cumulants involving single-sites and pairs, but treating higher-order cumulants approximately. The CG can be also used to include atomic correlations in the electronic structure

via the Korringa-Kohn-Rostoker (KKR) mulitple-scattering theory DCA,[48,49] which improves the ensemble averaging beyond the KKR CPA, which may provide a means to predict free energy and atomic short-range order directly in complex alloys.

ACKNOWLEDGMENTS

We thank V. I. Tokar for helpful exchanges. This work was funded by the National Science Foundation via Grants No. DMR-0705089 and No. DMR-03-25939 through the Materials Computation Center at Illinois. T.L.T. acknowledges a CSE Program Fellowship. D.D.J. received partial support from Ames Laboratory via the Department of Energy (Grant No. DE-AC02-07CH11358) through Iowa State University.

APPENDIX: CLUSTER FIELD-THEORY FORMALISM

The cluster field theory to solve for cluster $\hat{\Sigma}$, $\hat{G}$, and free energy is summarized. In vector notation, the partition function in (8) for the Ising Hamiltonian (1) on an N-site lattice, with m denoting N-site magnetizations, is separated into a product of single-site and pair terms as

$$Z[A] = e^{mA} Z_{\rm MF}[m] \det(2\pi G)^{1/2} e^{\frac{1}{2}AGA} R[AG]. \quad \text{(A1)}$$

$Z_{\rm MF}$ is $\exp(-\beta E_1)$, where E_1 is the single-site, mean-field energy (Sec. II), $\det(2\pi G)$ arises from factoring out the Gaussian part of the pair correlations, and A is the source field vector (see Tokar[15] for details). The last term, containing information beyond MFT and Gaussian fluctuations, is the generating functional of the S matrix[50] and is given by[15]

$$R[\phi] = \exp\left(\frac{1}{2}\partial_\phi G \partial_\phi\right) \exp\left[-\frac{1}{2}\phi\Sigma\phi + \beta(\bar{h} + mJ)\phi\right] \times \prod_i [\delta(\phi_i + m_i - 1) + \delta(\phi_i + m_i + 1)]. \quad \text{(A2)}$$

Delta functions arise due to the use of continuous-field variables rather than discrete variables ($\sigma_i = \pm 1$) for the derivation. From (9) and (A1), one deduces that

$$\left.\frac{\partial \ln R[AG]}{\partial A_i}\right|_{A=0} = 0, \quad \left.\frac{\partial^2 \ln R[AG]}{\partial A_i \partial A_j}\right|_{A=0} = 0. \quad \text{(A3)}$$

Setting $A = 0$ in (A1), the free energy $F = -k_B T \ln Z[0]$ is

$$F = E_1 - \frac{k_B T}{2} \ln\det(2\pi G) - k_B T \ln R[0], \quad \text{(A4)}$$

which is equivalent to Eq. (17) in Ref. 15. With no approximations in the derivation thus far, calculating $R[0]$ amounts to solving the Ising model exactly, which is only tractable in limited cases.

We use the CG methods described in the text that maintain Dyson's relation to build in the proper boundary conditions and the relation between cluster and lattice variables missing in the original theory. The CMFT divides the lattice into identical nonoverlapping, N_c-site clusters; i.e., pair correlations between sites of different clusters are ignored. With the cluster $\hat{\Sigma}$ and $\hat{G}$ given as $N_c \times N_c$ matrices, $R[AG]$ is decoupled into products of independent clusters (denoted by c), i.e.,

$$R[AG] \approx e^{-\beta(\bar{h}+mJ)m} \prod_{\rm c} \det(2\pi\hat{G})^{-1/2} \times e^{-\frac{1}{2}m(\hat{G}^{-1}+\hat{\Sigma})m} e^{-\frac{1}{2}A\hat{G}A - mA} \times \hat{Z}[A], \quad \text{(A5)}$$

with the cluster partition function given by

$$\hat{Z}[A] = {\rm Tr}_{\sigma\in c} \exp\left\{[m(\hat{G}^{-1} + \hat{\Sigma}) + \beta m J]\sigma \times -\tfrac{1}{2}\sigma(\hat{G}^{-1} + \hat{\Sigma})\sigma + \beta\bar{h}\sigma + A\sigma\right\}, \quad \text{(A6)}$$

where the trace is over N_c cluster sites with σ_i summed over the values -1 and $+1$. Hence, Eq. (A3) becomes

$$\hat{m}_i = \left.\frac{\partial \ln \hat{Z}[A]}{\partial A_i}\right|_{A=0}, \quad \hat{G}_{ij} = \left.\frac{\partial^2 \ln \hat{Z}[A]}{\partial A_i \partial A_j}\right|_{A=0}, \quad \text{(A7)}$$

from which the cluster $\hat{G}$ is obtained. The $\hat{G}$ thus derived satisfy (2) naturally for $i, j \in$ cluster.

Alternatively, by expressing the cluster partition function as $\hat{Z}[A] \equiv \exp[-\beta(\langle\hat{E}\rangle - T\hat{S})]$, we have expressed the cluster free energy derived from (A4) and (A5) more intuitively as in (28), where, for equivalent clusters, the cluster sum yields a factor of N/N_c (the number of clusters in the lattice). The cluster entropy is given by $\hat{S} = -k_B {\rm Tr}_{\sigma\in c}(P_\sigma \ln P_\sigma)$, which is separable into points, pairs, etc., within the cluster. For $N_c = 1$, (A7) yields (32) and (33).

The key to any cluster approximation is then to relate the cluster $\hat{G}$ and $\hat{\Sigma}$ to the correct lattice G and Σ in (3), as is done here via CG concepts from DCA and CDMFT, and use them in the correct cluster $\hat{Z}[A]$ for thermodynamics. For example, for a four-atom cluster, the trace in (A5) is evaluated for 16 configurations, which inherently includes multisite entropy.

*tantl@ihpc.a-star.edu.sg
†ddj@ameslab.gov

[1] N. A. Zarkevich and D. D. Johnson, Phys. Rev. Lett. **92**, 255702 (2004).
[2] N. A. Zarkevich, T. L. Tan, and D. D. Johnson, Phys. Rev. B **75**, 104203 (2007).
[3] V. Ozoliņš, C. Wolverton, and A. Zunger, Phys. Rev. B **57**, 6427 (1998).
[4] A. van de Walle and G. Ceder, Rev. Mod. Phys. **74**, 11 (2002).
[5] N. A. Zarkevich, T. L. Tan, L.-L. Wang, and D. D. Johnson, Phys. Rev. B **77**, 144208 (2008).
[6] L. Onsager, Phys. Rev. **65**, 117 (1944).
[7] G. Biroli, O. Parcollet, and G. Kotliar, Phys. Rev. B **69**, 205108 (2004).
[8] T. Maier, M. Jarrell, T. Pruschke, and M. H. Hettler, Rev. Mod. Phys. **77**, 1027 (2005).
[9] M. Jarrell and H. R. Krishnamurthy, Phys. Rev. B **63**, 125102 (2001).
[10] P. Soven, Phys. Rev. **156**, 809 (1967).
[11] D. W. Taylor, Phys. Rev. **156**, 1017 (1967).
[12] P. R. C. Kent, M. Jarrell, T. A. Maier, and T. Pruschke, Phys. Rev. B **72**, 060411 (2005).

[13]G. E. Stewart, D. D. Betts, and J. S. Flynn, J. Phys. Soc. Jpn. **66**, 3231 (1997).
[14]V. I. Tokar, Phys. Lett. A **110**, 453 (1985).
[15]V. I. Tokar, Comput. Mater. Sci. **8**, 8 (1997).
[16]P. Weiss, J. Phys. **6**, 661 (1907).
[17]W. Shockley, J. Chem. Phys. **6**, 130 (1938).
[18]L. Onsager, J. Am. Chem. Soc. **58**, 1486 (1936).
[19]J. B. Staunton and B. L. Györffy, Phys. Rev. Lett. **69**, 371 (1992).
[20]J. B. Staunton, D. D. Johnson, and F. J. Pinski, Phys. Rev. B **50**, 1450 (1994).
[21]R. Brout, Phys. Rev. **122**, 469 (1961).
[22]R. Brout, *Phase Transitions* (Benjamin, New York, 1965).
[23]Yu. A. Izyumov and Yu. N. Skryabin, *Statistical Mechanics of Magnetically Ordered Systems* (Consultants Bureau, New York, 1988).
[24]D. D. Johnson, J. B. Staunton, and F. J. Pinski, in *Methods in Materials Science*, edited by E. Kaufmann and J. Sanchez (Wiley, New York, 2000), pp. 2b.3.1–2b.3.27.
[25]I. Tsatskis, in *Local Structure from Diffraction* (Springer, New York, 2002), pp. 207–231.
[26]D. A. Rowlands, J. B. Staunton, and B. L. Györffy, Phys. Rev. B **67**, 115109 (2003).
[27]G. Baym, Phys. Rev. **127**, 1391 (1962).
[28]The MathWorks, Inc., MATLAB (R2008b), Natick, MA (2008).
[29]H. A. Bethe, Proc. R. Soc. London, Ser. A **150**, 552 (1935).
[30]Y. Y. Li, J. Chem. Phys. **17**, 447 (1949).
[31]F. Ducastelle, *Order and Phase Stability in Alloys* (North-Holland, New York, 1991).
[32]R. K. Pathria, *Statistical Mechanics* (Pergamon, New York, 1972).
[33]K. Binder, Phys. Rev. Lett. **45**, 811 (1980).
[34]A. D. Beath and D. H. Ryan, Phys. Rev. B **72**, 014455 (2005).
[35]P. C. Clapp and S. C. Moss, Phys. Rev. **171**, 754 (1968).
[36]P. C. Clapp and S. C. Moss, Phys. Rev. **142**, 418 (1966).
[37]G. S. Joyce, in *Phase Transitions and Critical Phenomena*, edited by C. Domb and M. S. Green (Academic, New York, 1972), Vol. 2, Chap. 10, pp. 375–442.
[38]R. V. Chepulskii and V. N. Bugaev, J. Phys. Condens. Matter **10**, 7309 (1998).
[39]V. I. Tokar and I. Tsatskis (unpublished).
[40]S. Katsura, T. Morita, S. Inawashiro, T. Horiguchi, and Y. Abe, J. Math. Phys. **12**, 892 (1971).
[41]G. N. Watson, Q. J. Math. **os-10**, 266 (1939).
[42]C. F. Baillie, R. Gupta, K. A. Hawick, and G. S. Pawley, Phys. Rev. B **45**, 10438 (1992).
[43]R. Gupta and P. Tamayo, e-print arXiv:cond-mat/9601048v1 (to be published).
[44]H. T. Diep, A. Ghazali, B. Berge, and P. Lallemand, Europhys. Lett. **2**, 603 (1986).
[45]S. Kämmerer, B. Dünweg, K. Binder, and M. d'Onorio de Meo, Phys. Rev. B **53**, 2345 (1996).
[46]M. E. Fisher, Rep. Prog. Phys. **30**, 615 (1967).
[47]V. I. Tokar,I. V. Masanskii, and T. A. Grishchenko, J. Phys. Condens. Matter **2** (1990).
[48]D. A. Biava, S. Ghosh, D. D. Johnson, W. A. Shelton, and A. V. Smirnov, Phys. Rev. B **72**, 113105 (2005).
[49]S. Ghosh, D. A. Biava, W. A. Shelton, and D. D. Johnson, Phys. Rev. B **73**, 085106 (2006).
[50]A. N. Vassiliev, *Functional Methods in Quantum Field Theory and Statistics* (Leningrad State University Press, Leningrad, 1976).